Supporting Information for CO_2, NO_x, and Particle Emissions from Aircraft and Support Activities at a Regional Airport

Michael E. Klapmeyer, Linsey C. Marr

EXPERIMENTAL METHODS

Mobile Flux Laboratory. The Flux Laboratory for the Atmospheric Measurement of Emissions (FLAME) is a modified television news van with an extendable mast that reaches 15 m above ground level. A sonic anemometer is mounted on a rotating boom at the top of the mast. Because the sonic anemometer is positioned on top of the mast and rotated into the direction of the prevailing wind, errors in measured wind velocities caused by aerodynamic shadowing of components are minimized. Conductive, 1.27-cm Teflon tubing (TELEFLEX T1618-08) is also mounted on the boom to convey air down to the instruments inside the FLAME. All instruments are secured in the vehicle's rear compartment, and a data logger (National Instruments Compact FieldPoint 2110) and computers record output from all analyzers at 10 Hz and process the data over 30-min intervals.

The mobile laboratory is powered using a 4.5-kW gasoline generator whose emissions are not expected to influence measurements under typical sampling conditions. Wind velocities below 0.2 m s-1 occurred less than 0.5% of the time. Given typical values of the vertical eddy diffusion coefficient under such conditions,[1,2] emissions from the mobile laboratory's onboard generator, whose exhaust was at ~0.5 m above ground level, would be transported at least ~1 m downwind in the time it would take them to disperse upward 15 m to the sample inlet. Thus, self-sampling of generator exhaust is expected to be negligible.

Table S1. Summary of seasonal sampling periods and temperature ranges.

season	dates		temperature (°C)		
	airfield	terminal	low	avg	high
summer	11 Jul 2011 18 Jul 2011 9 Aug 2011 10 Aug 2011	13 Jul 2011 8 Aug 2011 11 Aug 2011 15 Aug 2011	25.9	30.4	33.4
autumn	14 Oct 2011 21 Oct 2011 24 Oct 2011 27 Oct 2011	10 Nov 2011 11 Nov 2011 30 Nov 2011 2 Dec 2011	9.7	13.7	16.8
winter	13 Jan 2012 29 Jan 2012 30 Jan 2012 13 Feb 2012	18 Jan 2012 11 Feb 2012 12 Feb 2012 17 Feb 2012	0.3	4.0	7.6

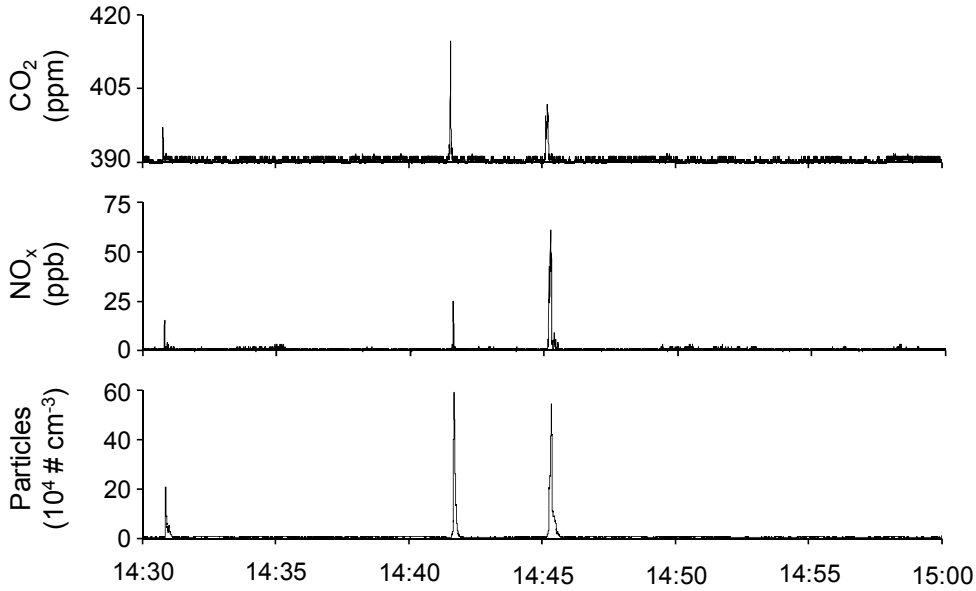

Figure S1. Example of aircraft exhaust plumes at 10-Hz resolution at the airfield. Three taxi and takeoff plumes from individual aircraft were clearly resolved against the background during the 30-min period shown.

QA/QC. Instruments were calibrated in accordance with manufacturers' recommendations prior to initiating measurements at each sampling location. In prior testing, sampling line losses with the 14-m long tubing used by the FLAME have been found to be negligible.[3] Since the particle number concentrations encountered in ambient air occasionally exceeded the particle counter's detection limit, sample flow to it was diluted by a factor of 10 with filtered, particle-free air, and measured values were subsequently increased by the same factor.

For eddy covariance calculations, spikes were identified through both visual inspection of the data as well as established statistical criteria and replaced by linear interpolation of good data.[4-6] In order to align the sonic anemometer's coordinate system with the local mean streamline winds, a planar-fit, three-dimensional coordinate rotation method was applied.[7] A lag correction was also applied, with the lag established by maximizing the cross-correlation between vertical wind velocity and each pollutant's concentration.[8,9] Time lags for CO_2, NO_x, and total particle number were found to be 7, 10, and 12 s, respectively.

Stationarity of key atmospheric variables is required to ensure the validity of calculated fluxes.[10,11] Stationarity was determined by calculating the difference between the average flux from a 30-min data set and the average of six consecutive 5-min sub-periods of the same 30-min period. If the difference between the two averages was greater than 60%, stationarity criteria were not satisfied and the flux from that given time period was excluded from further analysis.[12] In this campaign, the stationarity condition was achieved in 63% of the 30-min periods for CO_2, 69% for NO_x, and 63% for particle number.

Quality assurance also included spectral analysis, with spectra and co-spectra for temperature, vertical wind velocity, CO_2, NO_x, and particle number computed via Igor Pro's Power Spectral

Density and Cross Spectral Density functions. Frequency-weighted spectra and co-spectra, normalized by the variance and flux respectively, were plotted against dimensionless frequency, $n(z-z_d)/u$, where n is the natural frequency, $z - z_d$ is the difference between the measurement height and zero-plane displacement height, and u is the mean wind velocity. Figure S2 shows example spectra and co-spectra of temperature, CO_2, NO_x, and particle number along with the theoretically expected slopes of -2/3 and -4/3, respectively. The spectra and co-spectra of CO_2 indicated a frequency response similar to that of NO_x. This was due to an incorrect setting in the CO_2 analyzer's data filtering, discovered after the campaign, which led to response times that fell short of the instrument's capabilities.

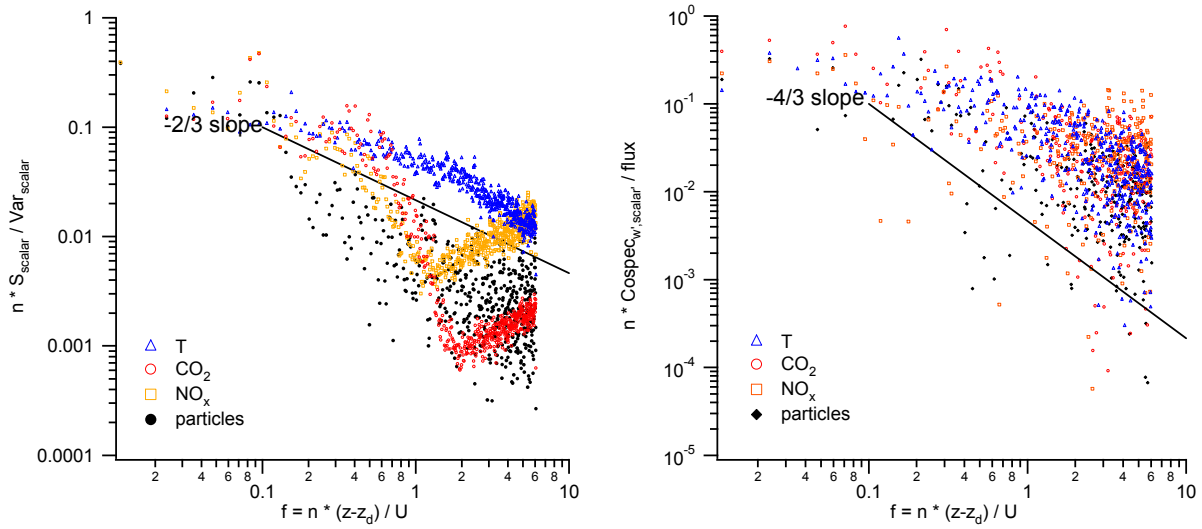

Figure S2. Example frequency-weighted spectra and co-spectra of temperature (T), CO_2, NO_x, and particle number, normalized by the variance or flux, respectively, and plotted against the normalized frequency.

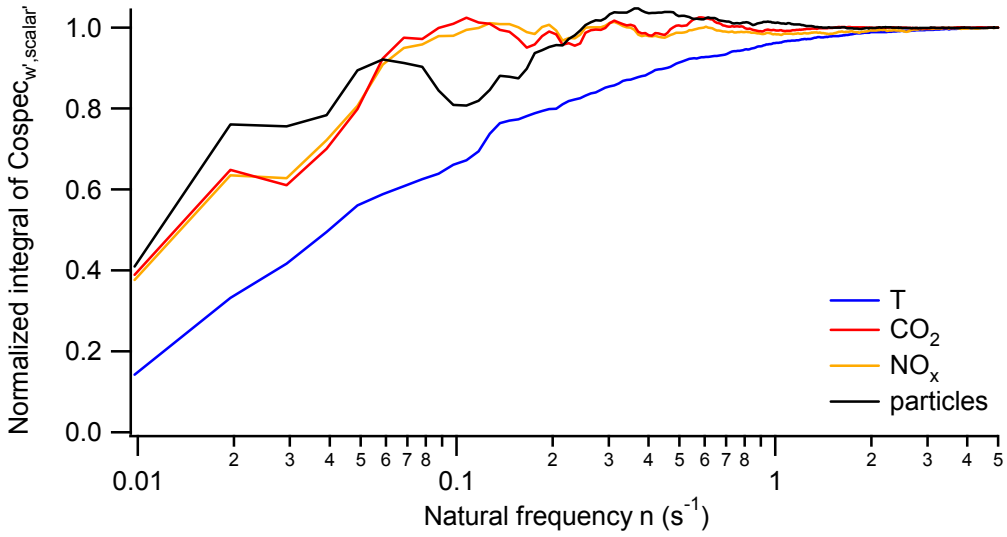

Figure S3. Example cumulative integral, normalized to the total, of the flux of temperature and NO_x as a function of the natural frequency. The data are from the same 30-min period as shown in Figure S2.

RESULTS

Concentrations. Table S2 shows average concentrations of CO_2, NO_x, particle number, and BC by season. Figures S3-S6 show boxplots of CO_2, NO_x, particle number, and BC at each sampling location. The vertical axis range is identical for each individual pollutant to facilitate comparisons between seasons and locations. Each time period (comprised of four separate data points, each representing a single day) is shown with box plots where the whiskers represent the minima and maxima values. Average seasonal concentrations are presented by dashed lines.

Table S2. Average (arithmetic mean) gaseous and particle concentrations during summer (S), autumn (A), and winter (W) sampling. Standard deviations of 30-min averages are shown in parentheses.

	CO_2 (ppm)			NO_x (ppb)			particle number (10^4 # cm^{-3})			BC ($\mu g\ m^{-3}$)		
location	S	A	W	S	A	W	S	A	W	S	A	W
airfield	378	396	401	4.6	6.1	4.0	0.6	2.6	3.7	0.6	0.6	0.3
	(14)	(16)	(5)	(5.6)	(11.3)	(4.5)	(0.5)	(1.6)	(2.5)	(0.4)	(0.6)	(0.2)
terminal	377	405	403	4.8	5.6	2.7	1.6	3.9	3.6	0.7	0.4	0.3
	(10)	(8)	(3)	(4.2)	(9.9)	(1.8)	(1.2)	(3.1)	(3.5)	(0.4)	(0.3)	(0.2)

Higher CO_2 concentrations, like those in excess of 460 ppm at the airfield in autumn, were not the result of fleeting aircraft activity, but rather very stable atmospheric conditions. These conditions typically occurred in the early morning hours and were followed by a steady decrease in concentrations as the mixing height rose and diluted the boundary layer. During these stable periods, self-sampling of the mobile laboratory's generator exhaust can be an issue, but horizontal winds speeds typically exceeded 1 m s^{-1}, high enough to render self-sampling extremely unlikely.

Fluxes. Figure S7 shows time series of fluxes of CO_2, NO_x, and particle number at both the airfield and terminal sites, combined over all three seasons. The figure also includes a zero line in red to easily distinguish between positive (upward) and negative (downward) fluxes. Because a number of 30-min periods failed to meet stationarity criteria, those with fewer than four valid data points are depicted by individual asterisks.

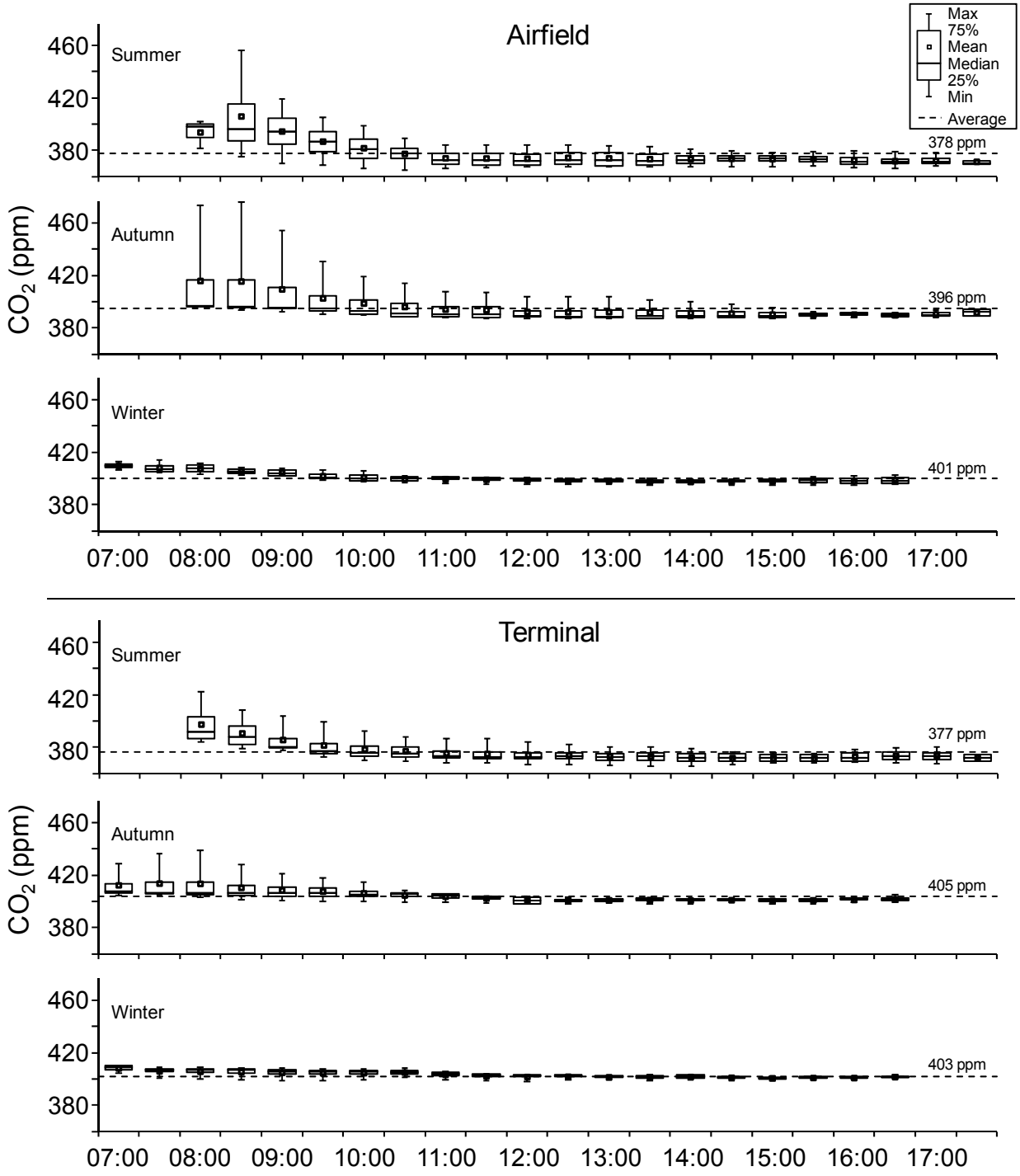

Figure S4. CO_2 time series at the airfield and terminal by season. The dashed lines represent the averages over all 30-min means at each site in each season.

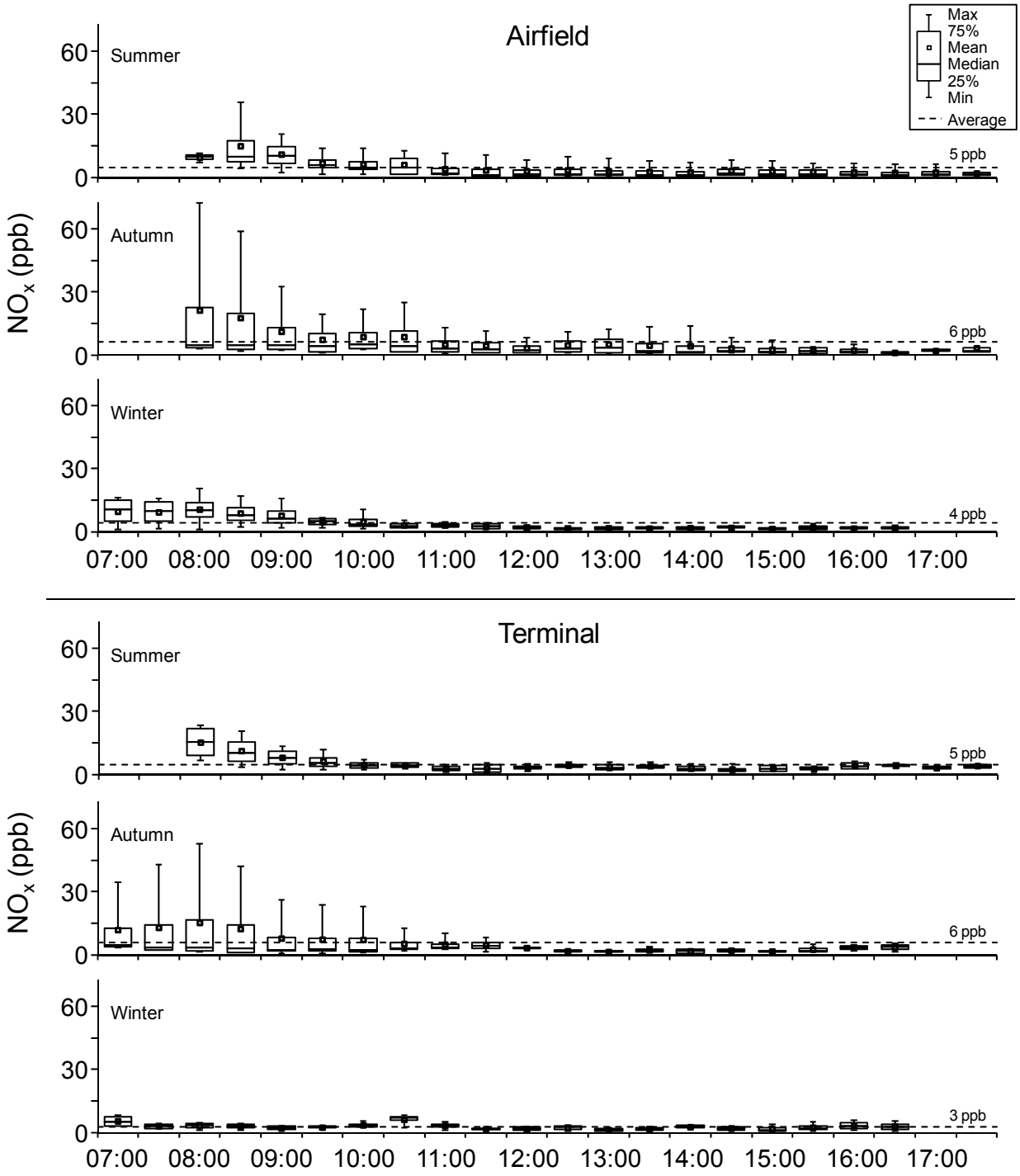

Figure S5. NO_x time series at the airfield and terminal by season. The dashed lines represent the averages over all 30-min means at each site in each season.

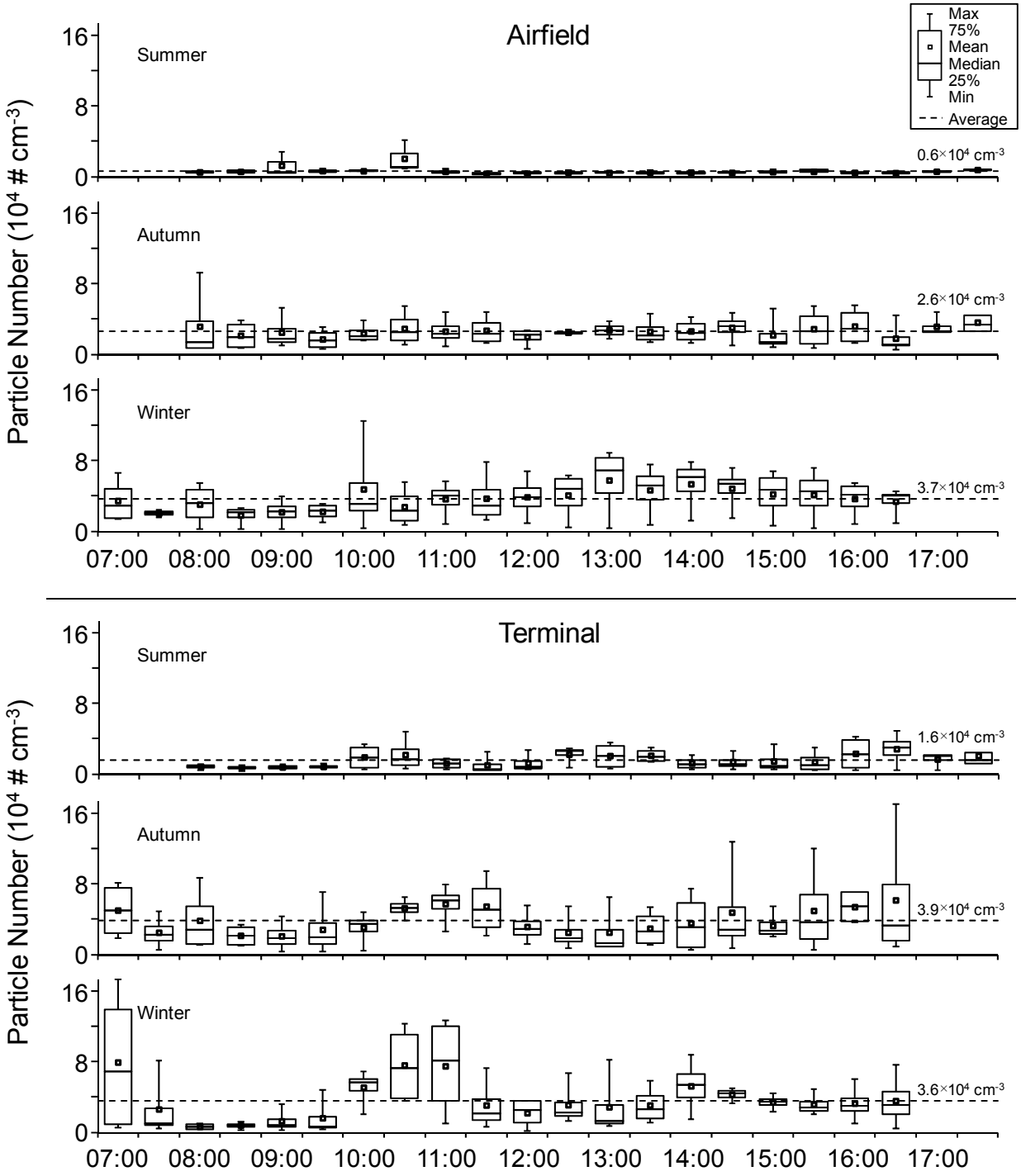

Figure S6. Particle number time series at the airfield and terminal by season. The dashed lines represent the averages over all 30-min means at each site in each season.

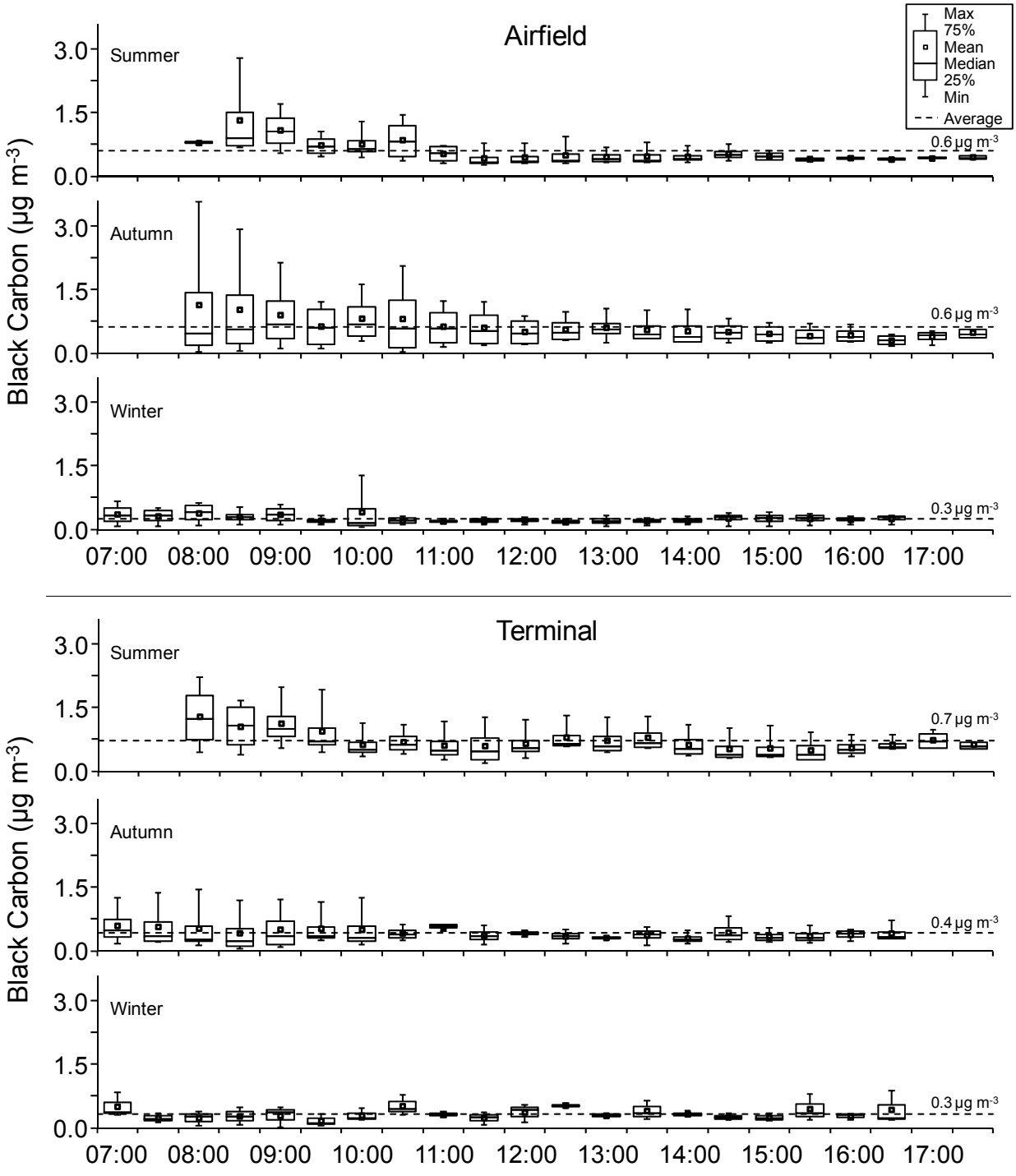

Figure S7. BC time series at the airfield and terminal by season. The dashed lines represent the averages over all 30-min means at each site in each season.

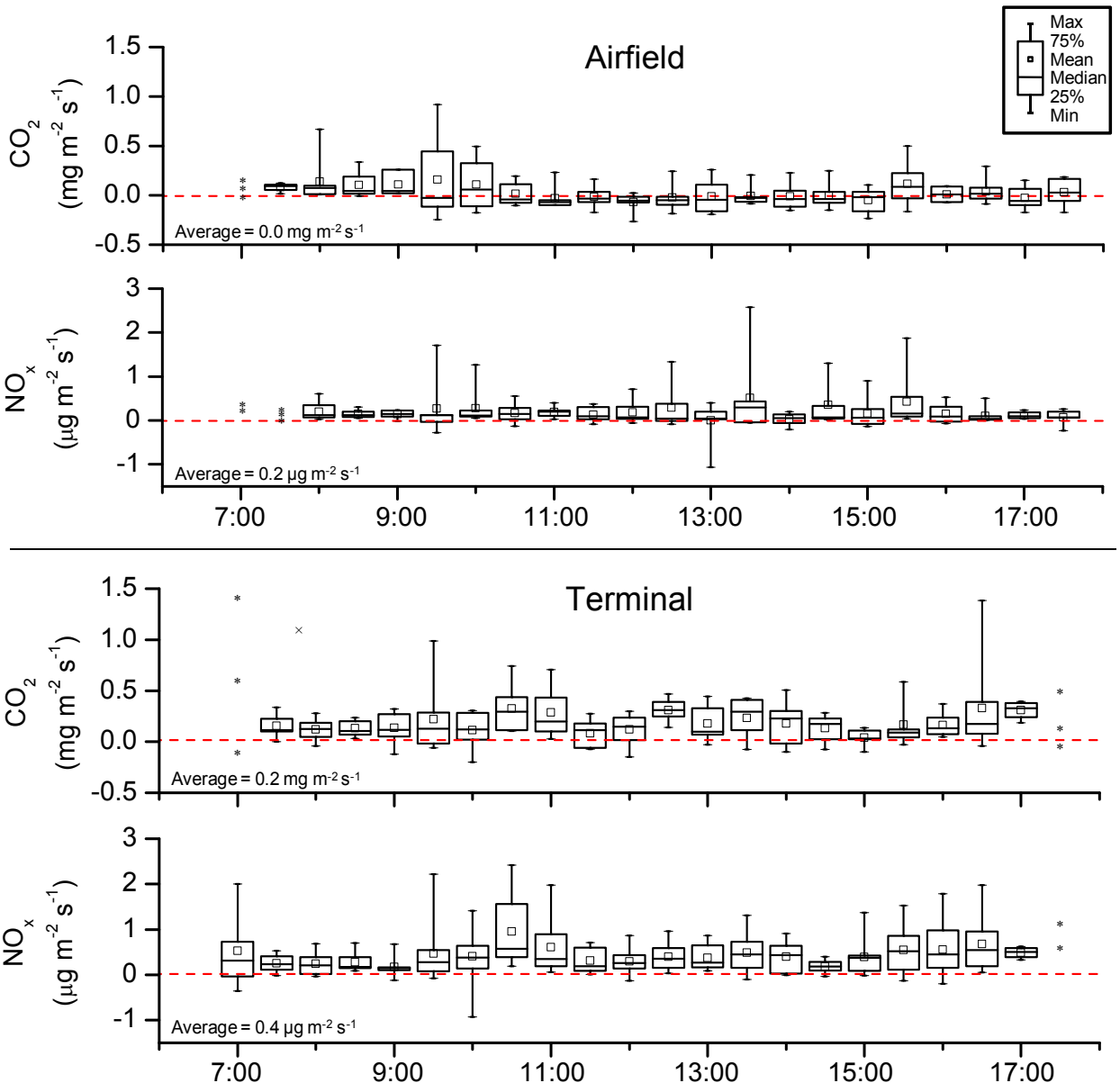

Figure S8. Time series of CO_2 and NO_x fluxes at the airfield and terminal. Asterisks indicate periods when fewer than four daily measurements were valid.

Table S3. NO_x EIs in this and other studies.

airport	aircraft[a]	mode	NO_x EI (g NO_2 kg^{-1})	reference
Roanoke, Virginia	regional/commuter/business	taxi/idle	2.2-4.0	This study
		takeoff	8.9-20.7	
Oakland, California and Cleveland, Ohio	Boeing 737, 757; Airbus A300; Embraer 145	taxi/idle	2.8-5	Timko et al., 2010[13]
		approach	6.5-11.8	
		climbout	10.4-24	
Heathrow, London	Boeing 747, 777; Airbus A320			
Atlanta, Georgia	various commercial jets	taxi/idle	3.3-4.0	Herndon et al., 2008[14]
		takeoff	7.2-22.0	
John F. Kennedy, New York	DC9, Airbus A320	taxi/idle	1.6-3.4	Herndon et al., 2004[15]
		takeoff	19-29	
Heathrow, London; Frankfurt; Vienna	various commercial jets	taxi/idle	1.4-2.7	Schäfer et al., 2003[16]
Heathrow, London	business jets to Boeing 747	taxi/idle	<5	Popp et al., 1999[17]
		taxi/idle	5-15	
		takeoff	15-52	

[a]These aircraft support a wide variety of engines. Specific engine models are available in some of the references cited.

Table S4. Particle number EIs in this and other studies.

airport	aircraft[a]	mode	particle number EI (# kg^{-1})	size cutoff[b]	reference
Roanoke, Virginia	regional/commuter/ business	taxi/idle	3.9-7.1 × 10^{15}	3 nm	this study
		takeoff	1.4-6.8 × 10^{15}	3 nm	
Santa Monica, California	commuter jets	takeoff	5 × 10^{16}	5.6 nm	Hu et al., 2009[18]
Atlanta, Georgia	various commercial jets	taxi/idle	4.0-8.2 × 10^{15}	7 nm	Herndon et al., 2008[14]
		takeoff	1.8-5.6 × 10^{15}	7 nm	
John F. Kennedy, New York	various commercial jets	taxi/idle	(2 ± 3) × 10^{14}	30 nm	Herndon et al., 2005[19]
		takeoff	(1 ± 0.7) × 10^{14}	30 nm	
Boston, Massachusetts		taxi/idle	(2.1 ± 1.1) × 10^{16}	7 nm	Herndon et al., 2005[19]
		takeoff	(8.8 ± 7.6) × 10^{15}	30 nm	

[a]These aircraft support a wide variety of engines. Specific engine models are available in some of the references cited.

[b]Minimum particle size detected by the particle counter employed.

Table S5. CO_2 fluxes in this and other studies.

location	land use	CO_2 flux ($mg\ m^{-2}\ s^{-1}$)	reference
Roanoke, Virginia	airport	0.1	This study
Münster, Germany	urban	0.2-0.5	41
Helsinki, Finland	urban	0.2	42
	vegetative cover	-0.1 in summer; 0.2 in winter	42
Mexico City	urban	0.4-0.8	22
Tijuana, Mexico	urban and suburban	0.4	11

REFERENCES

1. Seinfeld, J. H.; Pandis, S. N., *Atmospheric Chemistry and Physics - From Air Pollution to Climate Change*. Second ed.; John Wiley & Sons, Inc.: Hoboken, New Jersey, 2006
2. Stull, R. B., *An Introduction to Boundary Layer Meteorology*. Kluwer Academic Publishers: Dordrecht, The Netherlands, 1988.
3. Moore, T. O. Application of a mobile flux lab for the atmospheric measurement of emissions (FLAME). Ph.D. Dissertation, Virginia Tech, Blacksburg, VA, 2009.
4. Hojstrup, J., A statistical data screening procedure. *Measurement Science and Technology* **1993,** *4*, (2), 153-157; DOI doi:10.1088/0957-0233/4/2/003.
5. Schmid, H. P.; Grimmond, C. S. B.; Cropley, F.; Offerle, B.; Su, H.-B., Measurements of CO_2 and energy fluxes over a mixed hardwood forest in the mid-western United States. *Agricultural and Forest Meteorology* **2000,** *103*, (4), 357-374; DOI 10.1016/S0168-1923(00)00140-4.
6. Vickers, D.; Mahrt, L., Quality control and flux sampling problems for tower and aircraft data. *Journal of Atmospheric & Oceanic Technology* **1997,** *14*, (3), 512-526; DOI 10.1175/1520-0426(1997)014<0512:QCAFSP>2.0.CO;2.
7. Wilczak, J. M.; Oncley, S. P.; Stage, S. A., Sonic anemometer tilt correction algorithms. *Boundary-Layer Meteorology* **2001,** *99*, (1), 127-150; DOI 10.1023/A:1018966204465.
8. Leuning, R. A. Y.; Judd, M. J., The relative merits of open- and closed-path analysers for measurement of eddy fluxes. *Global Change Biology* **1996,** *2*, (3), 241-253; DOI 10.1111/j.1365-2486.1996.tb00076.x.
9. Nemitz, E.; Jimenez, J. L.; Huffman, J. A.; Ulbrich, I. M.; Canagaratna, M. R.; Worsnop, D. R.; Guenther, A. B., An eddy-covariance system for the measurement of surface/atmosphere

exchange fluxes of submicron aerosol chemical species - First application above an urban area. *Aerosol Science and Technology* **2008,** *42*, (8), 636-657; DOI 10.1080/02786820802227352.
10. Cullen, N. J.; Steffen, K.; Blanken, P. D., Nonstationarity of turbulent heat fluxes at Summit, Greenland. *Boundary-Layer Meteorology* **2007,** *122*, (2), 439-455; DOI 10.1007/s10546-006-9112-2.
11. Velasco, E.; Pressley, S.; Allwine, E.; Westberg, H.; Lamb, B., Measurements of CO_2 fluxes from the Mexico City urban landscape. *Atmospheric Environment* **2005,** *39*, (38), 7433-7446; DOI 10.1016/j.atmosenv.2005.08.038.
12. Aubinet, M.; Grelle, A.; Ibrom, A.; Rannik, U.; Moncrieff, J.; Foken, T.; Kowalski, A. S.; Martin, P. H.; Berbigier, P.; Bernhofer, C.; Clement, R.; Elbers, J.; Granier, A.; Grunwald, T.; Morgenstern, K.; Pilegaard, K.; Rebmann, C.; Snijders, W.; Valentini, R.; Vesala, T., Estimates of the annual net carbon and water exchange of forests: The EUROFLUX methodology. *Advances in Ecological Research* **2000,** *30*, 113-175.
13. Timko, M. T.; Herndon, S. C.; Wood, E. C.; Onasch, T. B.; Northway, M. J.; Jayne, J. T.; Canagaratna, M. R.; Miake-Lye, R. C.; Knighton, W. B., Gas turbine engine emissions-part I: volatile organic compounds and nitrogen oxides. *Journal of Engineering for Gas Turbines and Power-Transactions of the ASME* **2010,** *132*, (6); DOI 10.1115/1.4000131.
14. Herndon, S. C.; Jayne, J. T.; Lobo, P.; Onasch, T. B.; Fleming, G.; Hagen, D. E.; Whitefield, P. D.; Miake-Lye, R. C., Commercial aircraft engine emissions characterization of in-use aircraft at Hartsfield-Jackson Atlanta International Airport. *Environmental Science & Technology* **2008,** *42*, (6), 1877-1883; DOI 10.1021/es072029+.
15. Herndon, S. C.; Shorter, J. H.; Zahniser, M. S.; Nelson, D. D.; Jayne, J.; Brown, R. C.; Miake-Lye, R. C.; Waitz, I.; Silva, P.; Lanni, T.; Demerjian, K.; Kolb, C. E., NO and NO_2 emission ratios measured from in-use commercial aircraft during taxi and takeoff. *Environmental Science & Technology* **2004,** *38*, (22), 6078-6084; DOI 10.1021/es049701c.
16. Schäfer, K.; Jahn, C.; Sturm, P.; Lechner, B.; Bacher, M., Aircraft emission measurements by remote sensing methodologies at airports. *Atmospheric Environment* **2003,** *37*, (37), 5261-5271; DOI 10.1016/j.atmosenv.2003.09.002.
17. Popp, P. J.; Bishop, G. A.; Stedman, D. H., Method for commercial aircraft nitric oxide emission measurements. *Environmental Science & Technology* **1999,** *33*, (9), 1542-1544; DOI 10.1021/es981194+.
18. Hu, S.; Fruin, S.; Kozawa, K.; Mara, S.; Winer, A. M.; Paulson, S. E., Aircraft emission impacts in a neighborhood adjacent to a general aviation airport in Southern California. *Environmental Science & Technology* **2009,** *43*, (21), 8039-8045; DOI 10.1021/es900975f.
19. Herndon, S. C.; Onasch, T. B.; Frank, B. P.; Marr, L. C.; Jayne, J. T.; Canagaratna, M. R.; Grygas, J.; Lanni, T.; Anderson, B. E.; Worsnop, D.; Miake-Lye, R. C., Particulate emissions from in-use commercial aircraft. *Aerosol Science and Technology* **2005,** *39*, (8), 799-809; DOI 10.1080/02786820500247363.